Deuterium Solid-State NMR Study of the Dynamic Behavior of Deuterons and Water Molecules in Solid D$_3$PW$_{12}$O$_{40}$

Alexander G. Stepanov,*,[†,‡] Timur O. Shegai,[‡] Mikhail V. Luzgin,[†] Nadine Essayem,[§] and Hervé Jobic*,[§]

Boreskov Institute of Catalysis, Siberian Branch of the Russian Academy of Sciences,
Prospekt Akademika Lavrentieva 5, Novosibirsk 630090, Russia, Department of Natural Sciences,
Novosibirsk State University, Pirogova Street 2, Novosibirsk 630090, Russia, and
Institut de Recherches sur la Catalyse, CNRS, 2 av. Albert Einstein, 69626 Villeurbanne, France

Received: February 12, 2003

The mobility of water molecules and deuterons of the deuterated analogue of solid 12-tungstophosphoric acid, H$_3$PW$_{12}$O$_{40}$·nH$_2$O (HPA) (n = 5.5 and 0.1), has been characterized by deuterium solid-state NMR. Analysis of the ^{2}H NMR line shape and spin−lattice relaxation times allowed us to characterize the deuteron and water dynamics in HPA, at different water contents, in the temperature range 103−383 K. At 163−193 K and for n = 5.5, an intramolecular motion corresponding to reorientations by 180° flips around the C_2 axis of water in the [D$_5$O$_2$]$^+$ ion has been detected, the deuteron being probably immobile. At temperatures above 313 K, both water and deuteron become involved in fast rotation around the C_3 axis of the formed [D$_3$O]$^+$ ion. The rotation is performed on a time scale of 30−50 ns with an activation energy E_a of 8.5 kJ/mol. For n = 0.1, three dynamically different species can be distinguished: mobile deuterons, mobile [D$_3$O]$^+$ ions, and immobile deuterons. Mobile deuterons are weakly bonded to polyanions and move fast with a characteristic time of a few picoseconds and E_a = 8.6 kJ/mol. [D$_3$O]$^+$ ions move more slowly than deuterons, but still fast, with a time scale of a few nanoseconds, and E_a = 17.6 kJ/mol. The characteristic time for immobile deuterons is much greater than a few microseconds.

Introduction

Due to their high acidity, solid heteropolyacids (HPAs), such as 12-tungstophosphoric acid, H$_3$PW$_{12}$O$_{40}$, exhibit a high catalytic activity in acid-type reactions such as hydration, dehydration, alkylation, and isomerization.[1−5] In some cases, the reactions proceed in the "pseudoliquid phase",[2,4,6] where there are no separate catalytically active centers such as OH groups in zeolites. Protons play the role of active Brønsted acid centers in solid HPAs. Since the catalysts often contain water in the working state, the behavior of acidic protons in the presence of a small amount of water is an important subject. Hence the study of the dynamic behavior of protons and water is an essential part of investigations aiming to elucidate the molecular mechanism of catalytic acid−base type reactions occurring with solid HPAs.

The mobility of Brønsted sites in acidic zeolites has been well characterized by ^{1}H MAS NMR,[7,8] ^{2}H wide-line solid-state NMR,[9,10] and impedance spectroscopy,[11] whereas information about the dynamics of both protons and water in HPAs still remains scarce. Qualitative results about the rate of proton migration[8,12−15] and dynamics of water in H$_3$PW$_{12}$O$_{40}$·nH$_2$O[16] at temperatures below 373 K were reported, whereas quantitative information was reported only for water internal rotation in hexahydrate of HPA at 302−328 K[17] and for proton migration in anhydrous HPA at temperatures as high as 373 K.[18]

Deuterium solid-state NMR (^{2}H NMR) spectroscopy has been shown many times to be a powerful technique to characterize the Brønsted acid sites and to probe the dynamics of protons and water in zeolites,[9,10,19−21] intercalated in clay minerals,[22] in crystalline hydrates,[23,24] in cement systems,[25] on the surface of MCM-41,[26] in VPI-5 molecular sieve,[27] and in HPAs.[16,28] ^{2}H NMR is one of the experimental techniques providing information on the characteristics of the motional behavior of water molecules in solids. The line shape for ^{2}H NMR, being completely defined by intramolecular quadrupole interaction,[29−31] is especially sensitive to the mode of molecular motion and to its rate;[29,30] spin−lattice relaxation time is also dependent on the rate and mode of motion. The analysis of the dynamics is usually performed by simulating ^{2}H NMR line shape for different motional models until reasonable agreement with experiment is obtained. At the same time, by analyzing spin−lattice relaxation rates, one can also evaluate the nature of the molecular motion and its rate. Thus, peculiarities of the molecular motion of water and protons in acidic solids could be derived.

In this paper we use deuterium solid-state NMR that offers the promise of further quantitative characterization of the mobility of Brønsted acid sites and water in HPAs.

Experimental Section

Materials. Pure heteropolyacid H$_3$PW$_{12}$O$_{40}$ (HPA) sample was prepared according to the classical method including the synthesis of the sodium form, the extraction of H$_3$PW$_{12}$O$_{40}$ by diethyl ether, and the purification by recrystallization in water. Its BET surface was equal to 7 m^2 g^{-1}. Deuterated

* Corresponding authors. Fax: +7 3832 34 30 56; e-mail: a.g.stepanov@catalysis.nsk.su (A.G.S.). Fax: (33) 4 72 44 53 99; e-mail: jobic@catalyse.cnrs.fr (H.J.).
† Boreskov Institute of Catalysis.
‡ Novosibirsk State University.
§ Institut de Recherches sur la Catalyse.

12-tungstophosphoric acid was prepared as follows: H$_3$PW$_{12}$O$_{40}$·nH$_2$O was dissolved in D$_2$O. The solution was kept in a desiccator under Ar atmosphere to avoid any further exchange with atmospheric water protons. Then the deuterated HPA was recovered after complete evaporation of D$_2$O and its Keggin structure was checked by IR. The deuterium enrichment of the final product is 98%.

Sample Preparation. Two deuterated HPA samples were prepared for the NMR experiments by thermal treatment at 373 and 473 K for 2 h under nitrogen flow. According to TGA data, these two samples contain respectively 5.5 and 0.1 molecules of crystallization water per Keggin unit.[32] After cooling, a few grams of sample were transferred into a cylindrical glass tube of 5 mm o.d. and 3 cm length, this tube being connected to the Pyrex reactor used for the pretreatment under flowing nitrogen; the sample was then sealed off by flame. The tube was transferred into an NMR probe for recording the ^{2}H NMR spectra.

NMR Measurements. ^{2}H NMR experiments were performed at 61.42 MHz on a Bruker MSL-400 spectrometer, using a high power probe with 5 mm horizontal solenoid coil. All ^{2}H NMR spectra were obtained by Fourier transformation of the quadrature detected quadrupole echo, arising in a pulse sequence:[33]

$$\left(\frac{\pi}{2}\right)_{\pm X} - \tau_1 - \left(\frac{\pi}{2}\right)_Y - \tau_2 - \text{acquisition} - t \qquad \text{(i)}$$

where $\tau_1 = 30-50$ μs, $\tau_2 = 34-54$ μs, t is a repetition time for the sequence (i) during the accumulation of the NMR signal. The duration of the $\pi/2$ pulses was 1.6–5.0 μs. Spectra were typically obtained with 500–5000 scans and a repetition time of $t = 0.4-2$ s. Inversion–recovery experiments, to derive spin–lattice relaxation times (T_1), were carried out using the pulse sequence[34]

$$(\pi)_X - t_v - \left(\frac{\pi}{2}\right)_{\pm X} - \tau_1 - \left(\frac{\pi}{2}\right)_Y - \tau_2 - \text{acquisition} - t \qquad \text{(ii)}$$

where t_v was a variable delay between the 180° $(\pi)_X$ inverting pulse (as in standard inversion–recovery pulse sequence[34]) and the quadrupole echo sequence (i).

The temperature of the samples was controlled with a flow of nitrogen gas, stabilized with a variable-temperature unit BVT-1000 with a precision of about 1 K. The sample was allowed to equilibrate at least 15 min at a given temperature before the NMR signal was acquired.

Simulation of the NMR Spectra. ^{2}H NMR line shapes influenced by molecular motion were simulated based on the formalism described by Macho et al.[35] for two- and three-site exchange.

Theoretical Background

The ^{2}H NMR spectrum of deuterated polycrystalline water is dominated by quadrupole coupling.[29-31,36,37] This coupling is of intramolecular origin[29-31] and is strongly affected by the mode and the rate of the molecular motion in which the molecule is involved.[30,37,38]

For water molecules which are rigid on the ^{2}H NMR time scale, τ_{NMR} (i.e., when correlation times τ_C for molecular reorientation and internal motions satisfy the condition $\tau_C \gg \tau_{NMR} \sim Q_0^{-1} \approx 5 \times 10^{-6}$ s, where $Q_0 = C_Q^0 = e^2qQ/h$ is the quadrupole coupling constant unaffected by any motional averaging),[39] ^{2}H NMR spectra represent Pake-type powder patterns.[29,30] The dominant features of these line shapes are two strong peaks separated by the splitting $(3/4)Q_0$ and two shoulders
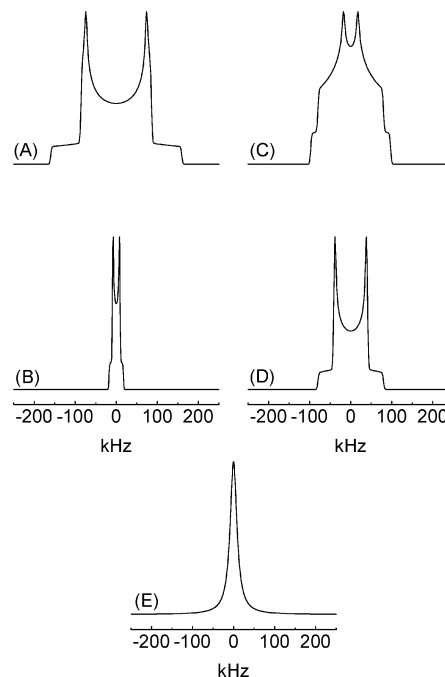

Figure 1. Simulated ^{2}H NMR line shapes for D$_2$O molecules within different motion regimes. (A) Static powder pattern for polycrystalline water, $C_Q^0 = 213$ kHz, $\eta = 0.074$; (B) fast rotation around the C_2 symmetry axis, with D−O−D angle $\gamma = 118.7°$; (C) π-flips around the C_2 symmetry axis with $\gamma = 118.7°$; (D) diffusion through the four positions shown in Figure 2; (E) isotropic reorientation.

separated by $(3/2)Q_0$ (see Figure 1A). For deuterium bonded to oxygen in polycrystalline water sample, Q_0 is about 213 kHz and the asymmetry parameter $\eta \sim 0.1$.[40,41]

If the O−D bond of the water molecule becomes involved in the motion, the line shape may be changed. The effect of this motion on the spectrum depends on the mode and rate of motion. For motions that are slow compared to $\tau_{NMR} \sim Q_0^{-1}$, no effect is observed in the spectrum. If, however, the correlation time τ_C approaches Q_0^{-1}, then the details of the motion will affect the shape of the spectrum.[42-44] While the powder line shape is very sensitive to the rates of motion between 10^3 and 10^7 s^{-1}, for faster motions, on a time scale of 10^8-10^{11} s^{-1}, the analysis of the spin−lattice relaxation times can be used to derive information about the mode and rate of the motional process.[23,45,46] Thus the analysis of the line shapes of the powder patterns and of the spin−lattice relaxation times can provide us information about the rate and mode of motion in which the water molecule is involved.

Let us analyze the possible motions of water molecules that may be encountered in the system under study. In H$_3$PW$_{12}$O$_{40}$·6H$_2$O, a secondary water structure has been described[47] with almost planar [H$_5$O$_2$]$^+$ ions, formed by two water molecules hydrogen bonded to a proton, where the bisector of the angle in both water molecules is collinear with the hydrogen bond. Analysis by X-ray and neutron scattering[47] has shown two possible mutually perpendicular directions for the ion orientation, as shown in Figure 2. The four water H atoms are hydrogen bonded to four oxygen atoms on four different Keggin units (polyanions), and different [H$_5$O$_2$]$^+$ ions lay on planes that are mutually orthogonal in a cubic lattice.

For the deuterated analogue of H$_3$PW$_{12}$O$_{40}$·6H$_2$O, the expected NMR signal will strongly depend on the details of water motion. In the case of fast π-flips around the C_2 symmetry axis, the resulting spectrum is biaxial with an effective quadrupole constant $C_Q = 130$ kHz and asymmetry parameter $\eta = 0.64$
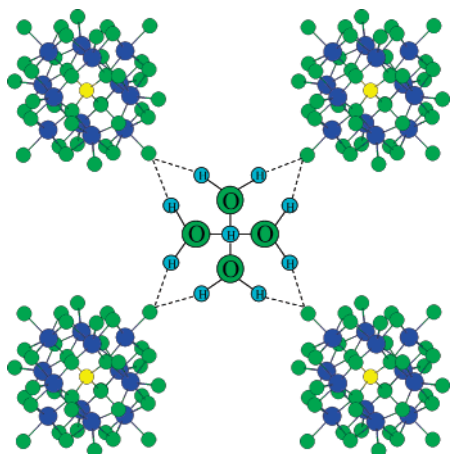
Figure 2. Water in the secondary structure of $H_3PW_{12}O_{40} \cdot 6H_2O$. Although two $[H_5O_2]^+$ ions are shown, there is only one at each site, with either of the two possible orientations shown, where water molecules occupy opposite positions. The four oxygen atoms shown in the external corners of the figure belong to four different Keggin cages.[47]

Figure 3. Variation with temperature of the ^2H NMR spectrum of $D_3PW_{12}O_{40} \cdot 5.5D_2O$. The deuterated HPA sample was heated for 2 h at 373 K under N_2 atmosphere.

Figure 4. ^2H NMR spectra for $[D_3O]^+$ ion, rapidly rotating around its C_3 axis: (A) experimental spectrum for $D_3PW_{12}O_{40} \cdot 5.5D_2O$ at 373 K; (B) simulated spectrum. The following parameters were taken for the simulation: $C_Q^0 = 213$ kHz as for rigid water, the D–O–D angle in $[D_3O]^+$ is 112°,[48] and the angle between the C_3 axis and the O–D direction is 109°.

for an angle γ between the two O–D bonds equal to 118.7° [47] (Figure 1B). In the case of fast reorientation of the $[D_5O_2]^+$ ion as a whole between two positions shown in Figure 2, the water molecule can be found with equal probability at any of the four positions, and the deuterium NMR spectrum would be an uniaxial Pake pattern with $C_Q = 106.5$ kHz (Figure 1C). If the water molecule undergoes fast free rotation around the C_2 symmetry axis, the resulting powder pattern is uniaxial with an effective quadrupole constant $C_Q = 23.5$ kHz (Figure 1D).

In a cubic lattice, the $[D_5O_2]^+$ ions shown in Figure 2 lay on planes that are normal to each other. If we imagine for water a fast diffusion throughout the cubic structure with $\tau_C \ll \tau_{NMR}$, then the quadrupole splitting is averaged to zero and a single line with a Lorentzian shape as shown in Figure 1E is observed at ω_I, the Larmor frequency of the deuterium nucleus.[31] The same kind of spectrum would be obtained from the central D atom in a $[D_5O_2]^+$ ion, as a consequence of the symmetry of the two hydrogen bonds which induces no electric field gradients.

Results and Discussion

Dynamics of Water and Deuterons in $D_3PW_{12}O_{40} \cdot 5.5D_2O$. Figure 3 shows the evolution with temperature of the ^2H NMR spectrum of deuterated HPA containing 5.5 water molecules per Keggin unit. At the lowest measured temperature of 104 K, the profile resembles that measured for rigid water molecules. The observed quadrupole constant $C_Q \sim 210$ kHz is only slightly reduced with respect to $C_Q = 213$ kHz[40,41] expected for rigid water. This can be related to the vibrational motion of water molecules hydrogen bonded to the oxygens of different Keggin units. The line shape for the spectra between 163 and 193 K is consistent with a π-flipping motion of the water molecules around their C_2 symmetry axis. The rate of this motion changes dramatically in this relatively narrow temperature range, as shown by simulations of the spectrum profile at different flipping rates (vide infra, Figure 5). The spectrum at 193 K corresponds to a rate of exchange of about 10^7 s^{-1}; a further increase of the exchange rate would not affect the line shape for this motion.

A further increase of the temperature to 318 K results in spectra that can hardly be assigned to simple modes of water or deuteron motion. One can assume that at least two additional signals, besides that assigned to the π-flips, contribute to the
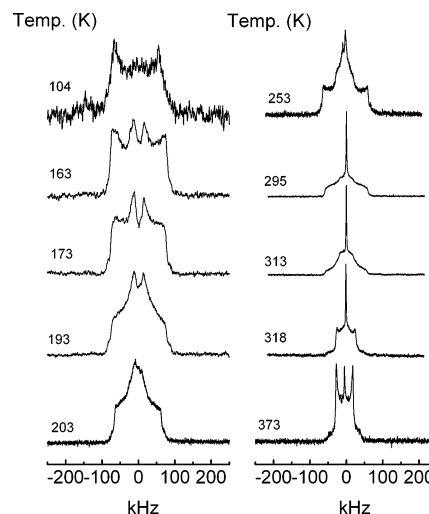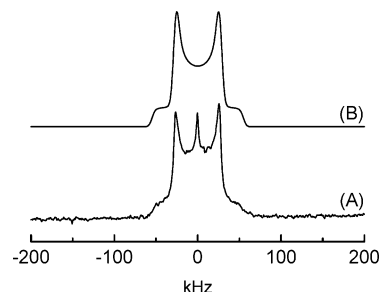
total NMR spectrum. The appearance of the narrow Lorentzian-type signal with a line width of about 1600 Hz indicates that parts of water and/or deuterons become involved in isotropic motions in the secondary structure of HPA. The last signal, whose structure is not clear up to 318 K, converts to a uniaxial powder pattern at $T > 313$ K, narrowed compared to that expected for rigid water. This signal with quadrupole constant $C_Q = 74$ kHz and $\eta \sim 0$ prevails in the spectrum at temperatures above 318 K.

An analysis of the possible modes for this motion in which water molecules and deuterons could be involved in $[D_5O_2]^+$ in the secondary structure of HPA, and for which uniaxial powder patterns should be expected (see Figure 1), has not shown any correspondence to the spectrum experimentally observed at temperatures above 313 K.

Another possibility of existence of water and deuterons in the secondary structure of HPA is the $[D_3O]^+$ ion.[15] A fast uniaxial rotation of the $[D_3O]^+$ ion around its C_3 axis can provide the uniaxial powder pattern observed at temperatures above 318 K. Indeed, assuming the known geometry of the $[D_3O]^+$ ion[48] and fast free diffusion around its C_3 axis, a good correspondence between experimental and simulated spectra is obtained (Figure 4).

We have also performed simulations of the spectra for water motion, consistent with a π-flipping motion of the molecule around its C_2 symmetry axis, with the aim to estimate the rate of this motion. Experimental and simulated spectra are shown
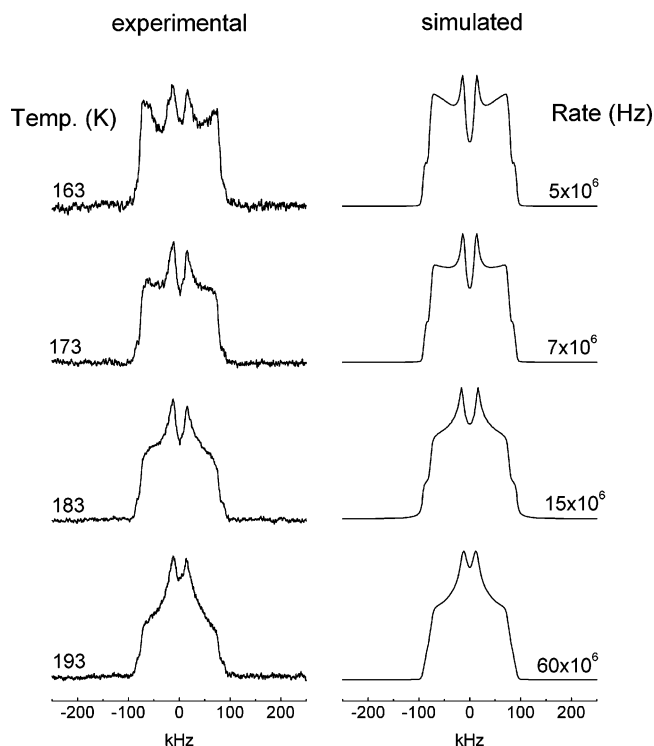
Figure 5. Experimental and simulated ^{2}H NMR spectra for D$_3$PW$_{12}$O$_{40}$·5.5D$_2$O in the range 163−193 K. The model of π-flipping motion of the molecule around its C_2 symmetry axis was used. The D−O−D angle in the water molecule was assumed to be 118.7°. Simulations were performed for τ = 54 μs; C_Q^0 = 213 kHz and η = 0.074 for rigid water molecules. The hopping rates used in the simulation are shown near each spectrum.
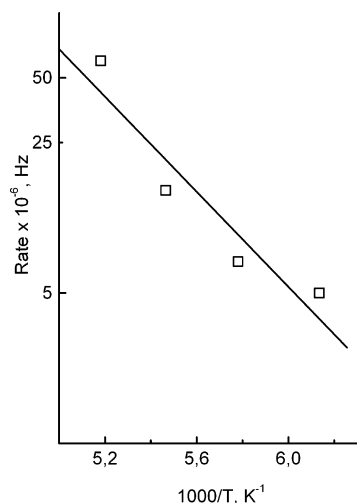

Figure 6. Observed temperature dependence of jump rate for the π-flipping motion of the water molecule in D$_3$PW$_{12}$O$_{40}$·5.5D$_2$O in the temperature range 163−193 K. A least-squares fit of the data yields an activation energy of 21 ± 5 kJ/ mol.

in Figure 5. An Arrhenius plot of the estimated rates for this π-flipping motion shows that the activation energy for this process is about 21 kJ/mol (Figure 6). Water molecules can be considered here as twice hydrogen bonded to the Keggin unit oxygens. Therefore, it is no wonder that the activation energy is typical for hydrates with hydrogen bonds of moderate strength if crossing the rotational barrier is associated with breaking of the hydrogen bonds.[23,41,49] As a further support of our measurements note that this type of water motion in the hexahydrate of HPA was reported earlier by the QENS technique, with similar dynamic characteristics but at higher temperatures (302−328
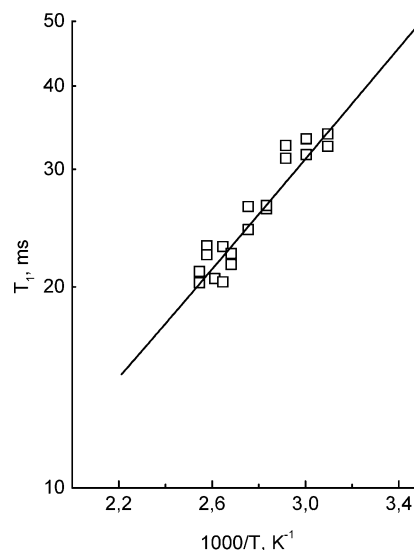

Figure 7. Temperature dependence of ^{2}H NMR spin−lattice relaxation time for the narrowed uniaxial powder pattern observed for D$_3$PW$_{12}$O$_{40}$·5.5D$_2$O at 318−373 K. The solid line represents a fit to the experimental points based on the model for continuous diffusion about a symmetry axis by Torchia and Szabo[45] with the following effective parameters: C_Q^0 = 213 kHz, τ_o = 2 ns, E_a = 8.5 kJ/mol; the angle between the O−D direction and the rotational C_3 axis is equal to 109°. Only a contribution to T_1 at perpendicular edges of the powder pattern was taken into account.

K).[17] The activation energy provided by QENS for a π-flip motion of the water molecule was 14 kJ/mol.[17] Taking into account the isotope effect for deuterium, E_a(D) $\approx$ E_a(H) + 0.15$h\nu_{OH}$, the activation energy for deuterated water should be higher by about 6.5 kJ/mol. Consequently, E_a(H) = 21 − 6.5 = 14.5 kJ/mol is in good agreement with the activation energy found in ref 17.

The fate of a deuteron in [D$_5$O$_2$]$^+$, when the water molecules are involved in π-flipping motion, is unclear. It would be reasonable to assume that the deuteron should be immobile and some additional signal should be observed in Figure 1 at 163−193 K, besides the signal of water molecules exhibiting π-flips. The absence of this weak signal allows us to assume that the signal is broad and is not identified in the spectrum.

To estimate the rate for the rotational motion of the [D$_3$O]$^+$ ion around its C_3 axis, we further analyzed spin−lattice relaxation times for the narrowed uniaxial powder pattern observed between 318 and 373 K. The variation of the logarithm of T_1 versus reciprocal temperature is linear through the whole temperature range studied (Figure 7). The slope of T_1 indicates that we are operating far from the T_1 minimum, and that the quadrupole spin−lattice relaxation time is defined by the slow internal motion with characteristic correlation times τ_C satisfying the condition $\omega_I \tau_C \gg 1$, i.e., $\tau_C \gg 2.6 \times 10^{-9}$ s. A fit to the experimental points with the expression for T_1 by Torchia and Szabo[45] for free continuous diffusion of [D$_3$O]$^+$ around the C_3 axis allowed us to estimate the preexponential factor, τ_0 = 2 ns, and the activation energy E_a = 8.5 kJ/mol for this motion. The estimated activation energy is essentially less than that expected if crossing the rotational barrier would be associated with breaking the hydrogen bonds. Therefore, we conclude that the [D$_3$O]$^+$ ion is indeed involved in a rotational diffusion process and is weakly bound to the oxygens of the Keggin units.

It is interesting to note that the rate of the [D$_3$O]$^+$ ion free diffusion at 318−373 K is $\sim$(2−3) $\times$ 10^7 s^{-1}, which is of the same order of magnitude as the π-flips of water molecules at lower temperature. However, water molecules are hydrogen
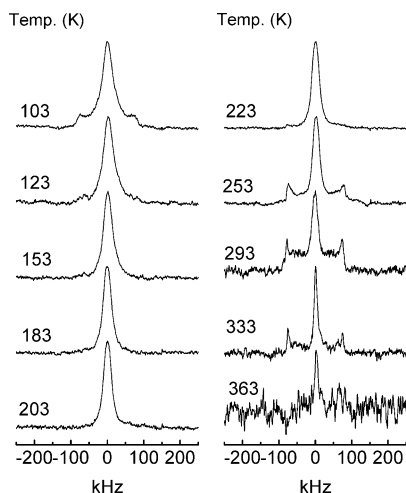
Figure 8. Variation with temperature of the ^{2}H NMR spectrum of D$_3$PW$_{12}$O$_{40}$·0.1D$_2$O. The deuterated HPA sample was heated for 2 h at 473 K under N$_2$ atmosphere.

bonded while performing π-flips, whereas the hydrogen bonding may be substantially weakened for a rotating [D$_3$O]$^+$ ion.

It should also be noted that while protonated water is involved in fast rotational diffusion in the form of [D$_3$O]$^+$ ion at $T >$ 313 K, the other water molecule from [D$_5$O$_2$]$^+$ remains invisible by NMR, the signal attributed to [D$_3$O]$^+$ prevailing at $T >$ 313 K (Figure 3). Here we can only suggest that the motion of these water molecules is performed with rates that do not allow detection of this signal with the solid echo sequence (i). In quadrupole echo experiments, a significant attenuation of the echo can be observed, if a molecule reorientational correlation time τ_C satisfies the condition $\omega_I \tau_C \gg 1$ (see, e.g., ref 23).

Dynamics of Water and Deuterons in D$_3$PW$_{12}$O$_{40}$·0.1D$_2$O. Figure 8 shows the evolution with temperature of the ^{2}H NMR spectrum for deuterated HPA, containing only 0.1 molecule of water per unit cell, so that mainly isolated deuterons are present in the system. According to ^{1}H MAS NMR and neutron scattering studies, this sample contains also a small amount of hydroxonium ions.[32,50] A liquidlike line shape is preferentially observed at 103−233 K. At temperatures above 253 K a solidlike pattern with C_Q = 210 kHz contributes also to the total ^{2}H NMR spectrum. The prevalence of the liquidlike line shape indicates that the motion is basically isotropic. It may correspond to the migration of the deuterons and [D$_3$O]$^+$ ions among neighbor polyanions in the secondary structure of HPA or to random hops among different oxygens of a single Keggin unit.

The analysis of the spin−lattice relaxation time for the liquidlike signal reveals two minima in the temperature dependence of T_1 (Figure 9). The first minimum is observed at ca. 260 K, and the second one is below 180 K. Such a dependence can be caused by the presence of two different modes of motion in which the deuterons are involved. This T_1 dependence can be described using the model of isotropic reorientation with two contributions:[51]

$$\frac{1}{T_1} = Af(\omega_I, \tau_{C1}) + Bf(\omega_I, \tau_{C2}) \quad (1)$$

$$f(\omega, \tau) = g(\omega, \tau) + 4g(2\omega, \tau)$$

$$g(\omega, \tau) = \frac{\tau}{1 + \omega^2 \tau^2}$$

Here, the coefficients A and B determine the contribution of the different motions to the total relaxation. A and B are linked
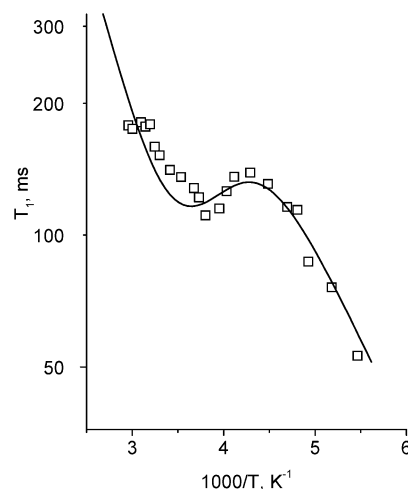

Figure 9. Temperature dependence of the ^{2}H NMR spin−lattice relaxation time for D$_3$PW$_{12}$O$_{40}$·0.1D$_2$O in the range 318−373 K. The solid line represents a fit to the experimental points based on the model of two contributions to T_1 (eq 1) and using the following effective parameters: $A = 1.23 \times 10^8$ Hz^2, $B = 0.0168 \times 10^8$ Hz^2; $E_{a1} = 8.6$ kJ/mol, $\tau_{01} = 0.1$ ps, $E_{a2} = 17.6$ kJ/mol, and $\tau_{02} = 1$ ps.

by the relation $A + B = \omega_Q^2$, where $\omega_Q = (3/4)C_Q^{\text{eff}}$, C_Q^{eff} is the effective quadrupole constant, which is dependent on the rate and type of the movement; τ_{C1} and τ_{C2} are the correlation times for the two different modes of motion.

Assuming an Arrhenius type dependence for the correlation times τ_{C1} and τ_{C2} vs temperature, $\tau = \tau_0 \exp(E_a/RT)$, the T_1 dependence was fitted using eq 1. Two sets of parameters E_a and τ_0 were derived: $E_{a1} = 8.6$ kJ/mol and $\tau_{01} = 0.1$ ps, and $E_{a2} = 17.6$ kJ/mol, $\tau_{02} = 1$ ps. These parameters correspond to the two modes of motion with characteristic times of 3 and 1200 ps at 300 K.

It should be noted that the contribution of the second mode of motion to the total T_1 is only about 1%; the faster motion prevails. If we assume that all remaining water molecules that are present in the system are protonated and exist in the form of [D$_3$O]$^+$ ions, then the quantity does not exceed 3%. This implies that we can assign the faster motion to the deuterons and the slower motion to the [D$_3$O]$^+$ ions. Both modes of motion can correspond either to hops of [D$_3$O]$^+$ ions and deuterons among the oxygen atoms within one polyanion or to hops between neighboring polyanions. Note that the deuterons are rather weakly bound to the oxygens of polyanions if we assume that the activation energy of 8.6 kJ/mol relates to the energetic barrier for breaking the bond between the oxygens of polyanions and deuterons. This is essentially less than E_a for water reorientation in crystallohydrates, when this reorientational motion is related to hydrogen bond breaking.[52] The activation energy of 17.6 kJ/mol for the [D$_3$O]$^+$ ion motion seems to be related to the energy barrier necessary for breaking the hydrogen bond between a deuteron of the [D$_3$O]$^+$ ion and the oxygens of polyanions. This activation energy is close to E_a for water reorientation by π-flipping in HPA containing 5.5 water molecules per Keggin unit (vide supra). This is indicative of a similar strength of hydrogen bonding for water and [D$_3$O]$^+$ ion in HPA.

Uchida et al.[15] estimated the rate of migration for a proton between the polyanions at about 200 Hz. It follows from our data that this migration can be performed with a faster rate.

The Pake powder pattern which contributes also to the total spectrum, besides the liquidlike line shape (Figure 8, $T >$ 253 K), indicates that some part of the deuterons is comparatively immobile. They move with a rate essentially less than the

observed quadrupole splitting of about 210 kHz, i.e., on a time scale longer than 4.7×10^{-6} s. These deuterons seem to be strongly bonded to the oxygens of the polyanions and exist in the form of OD groups.

Thus, for deuterated H$_3$PW$_{12}$O$_{40}$·0.1H$_2$O, three dynamically different species can be distinguished with ^{2}H NMR: mobile deuterons, mobile [D$_3$O]$^+$ ions, and immobile deuterons. Mobile deuterons are weakly bonded to polyanions and move fast on the time scale of a few picoseconds; mobile [D$_3$O]$^+$ ions move more slowly than deuterons, but still fast with a time of a few nanoseconds. The characteristic time for immobile deuterons is much longer than microseconds.

Conclusion

An analysis of the temperature dependence of the ^{2}H NMR line shape and spin−lattice relaxation times of the *deuterated* analogue of solid 12-tungstophosphoric acid, H$_3$PW$_{12}$O$_{40}$·nH$_2$O (HPA) ($n = 5.5$ and 0.1), allowed us to draw the following conclusions about the peculiarities of deuteron and water dynamics in the range 103−383 K. At 163−193 K and $n = 5.5$, an intramolecular motion has been detected, representing a reorientation of the water molecule by π-flips around its C_2 axis in the [D$_5$O$_2$]$^+$ ion. At temperatures above 313 K, both water and deuteron are involved in fast rotation around a C_3 axis in the formed [D$_3$O]$^+$ ion. The rotation is performed on a time scale of 30−50 ns, with an activation energy of 8.5 kJ/mol, indicating weak hydrogen bonding of the ion with the oxygens of HPA. For $n = 0.1$, three dynamically different species can be distinguished in the range 173−363 K: mobile deuterons, mobile [D$_3$O]$^+$ ions, and immobile deuterons. Mobile deuterons are weakly bonded to polyanions and move fast with a characteristic time of 3−40 ps and $E_a = 8.6$ kJ/mol. [D$_3$O]$^+$ ions move more slowly than deuterons, but still fast within the time 0.3−200 ns and $E_a = 17.6$ kJ/mol. Immobile deuterons can only move with a characteristic time much greater than microseconds.

References and Notes

(1) Kozhevnikov, I. V. *Russ. Chem. Rev.* **1987**, *6*, 811.

(2) Misono, M. *Catal. Rev.−Sci. Eng.* **1987**, *29*, 269.

(3) Okuhara, T.; Mizuno, N.; Misono, M. *Adv. Catal.* **1996**, *41*, 113−252. Shikata, S.; Okuhara, T.; Misono, M. *J. Mol. Catal. A: Chem.* **1995**, *100*, 49−59. Kozhevnikov, I. V. *Catal. Rev.−Sci. Eng.* **1995**, *37*, 311.

(4) Misono, M. *Catal. Rev.−Sci. Eng.* **1988**, *30*, 339.

(5) Okuhara, T.; Na, K.; Misono, M. *Stud. Surf. Sci. Catal.* **1995**, *92*, 245−250. Essayem, N.; Kieger, S.; Coudurier, G.; Vedrine, J. C. *Stud. Surf. Sci. Catal.* **1996**, *101A*, 591−600. Essayem, N.; Coudurier, G.; Fournier, M.; Vedrine, J. C. *Catal. Lett.* **1995**, *34*, 223. Guisnet, M.; Bichon, P.; Gnep, N. S.; Essayem, N. *Top. Catal.* **2000**, *11/12*, 247−254.

(6) Misono, M.; Sakata, K.; Yoneda, Y.; Lee, W. Y. *Proceedings of the 7th International Congress on Catalysis*; Kodansha: Tokyo, 1980; Elsevier: Amsterdam, 1981; p 1047.

(7) Koller, H.; Engelhardt, G.; van Santen, R. A. *Top. Catal.* **1999**, *9*, 163−180. Baba, T.; Komatsu, N.; Ono, Y.; Sugisawa, H.; Takahashi, T. *Microporous Mesoporous Mater.* **1998**, *22*, 203−210. Sarv, P.; Tuherm, T.; Lippmaa, E.; Keskinen, K.; Root, A. *J. Phys. Chem.* **1995**, *99*, 13763−13768. Ernst, H.; Freude, D.; Mildner, T.; Pfeifer, H. In *12th International Zeolite Conference, 1998*; Treacy, M. M. J., Ed.; Materials Research Society: Warrendale, 1999; Vol. 4, pp 2955−2962.

(8) Baba, T.; Ono, Y. *Appl. Catal. A: Gen.* **1999**, *181*, 227−238.

(9) Vega, A. J.; Luz, Z. *J. Phys. Chem.* **1987**, *91*, 365−373.

(10) Kobe, J. M.; Gluszak, T. J.; Dumesic, J. A.; Root, T. W. *J. Phys. Chem.* **1995**, *99*, 5485−5491.

(11) Franke, M. E.; Simon, U. *Solid State Ionics* **1999**, *118*, 311−316.

(12) Baba, T.; Ono, Y. *J. Phys. Chem.* **1996**, *100*, 9064−9067.

(13) Baba, T.; Hasada, Y.; Nomura, M.; Ohno, Y.; Ono, Y. *J. Mol. Catal. A: Chem.* **1996**, *114*, 247−255.

(14) Uchida, S.; Inumaru, K.; Dereppe, J. M.; Misono, M. *Chem. Lett.* **1998**, 643−644.

(15) Uchida, S.; Inumaru, K.; Misono, M. *J. Phys. Chem. B* **2000**, *104*, 8108−8115.

(16) Chidichimo, G.; Golemme, A.; Imbardelli, D.; Santoro, E. *J. Phys. Chem.* **1990**, *94*, 6826−6830.

(17) Pressman, H. A.; Slade, R. C. T. *Chem. Phys. Lett.* **1988**, *151*, 354−361.

(18) Chuvaev, V. F.; Popov, K. I.; Spitsin, V. I. *Dokl. Akad. Nauk SSSR* **1980**, *255*, 892−895.

(19) Freude, D.; Ernst, H.; Wolf, I. *Solid State NMR* **1994**, *3*, 271−286.

(20) Luz, Z.; Vega, A. J. *J. Phys. Chem.* **1987**, *91*, 374−382.

(21) Ishimaru, S.; Ikeda, R. *Z. Naturforsch., A: Phys. Sci.* **1997**, *52*, 863−866.

(22) Ishimaru, S.; Ikeda, R. *Z. Naturforsch., A: Phys. Sci.* **1999**, *54*, 431−436.

(23) Long, J. R.; Ebelhaeuser, R.; Griffin, R. G. *J. Phys. Chem. A* **1997**, *101*, 988−994.

(24) Mizuno, M.; Hamada, Y.; Kitahara, T.; Suhara, M. *J. Phys. Chem. A* **1999**, *103*, 4981−4985.

(25) Rakiewicz, E. F.; Benesi, A. J.; Grutzeck, M. W.; Kwan, S. *J. Am. Chem. Soc.* **1998**, *120*, 6415−6416.

(26) Hwang, D. W.; Sinha, A. K.; Cheng, C.-Y.; Yu, T.-Y.; Hwang, L.-P. *J. Phys. Chem. B* **2001**, *105*, 5713−5721.

(27) Duer, M. J.; He, H. Y.; Kolodziejski, W.; Klinowski, J. *J. Phys. Chem.* **1994**, *98*, 1198−1204.

(28) Di Benedetto, S.; Chidichimo, G.; Golemme, A.; Imbardelli, D. *J. Phys. Chem.* **1996**, *100*, 8079−8084.

(29) Mehring, M. In *NMR Basic Principles and Progress*; Diehl, P., Fluck, E., Kosfeld, R., Eds.; Springer-Verlag: New York, 1976; Vol. 11.

(30) Spiess, H. W. In *NMR Basic Principles and Progress*; Diehl, P., Fluck, E., Kosfeld, R., Eds.; Springer-Verlag: New York, 1978; Vol. 15; p 55.

(31) Abragam, A. *The Principles of Nuclear Magnetism*; Oxford University Press: Oxford, 1961.

(32) Essayem, N.; Tong, Y. Y.; Jobic, H.; Vedrine, J. C. *Appl. Catal. A* **2000**, *194−195*, 109−122.

(33) Powles, J. G.; Strange, J. H. *Proc. Phys. Soc.* **1963**, *82*, 6. Davis, J. H.; Jeffery, K. R.; Bloom, M.; Valic, M. I.; Higgs, T. P. *Chem. Phys. Lett.* **1976**, *42*, 390−394.

(34) Farrar, T. C.; Becker, E. D. *Pulse and Fourier Transform NMR. Introduction to Theory and Methods*; Academic Press: New York and London, 1971.

(35) Macho, V.; Brombacher, L.; Spiess, H. W. *Appl. Magn. Reson.* **2001**, *20*, 405−432.

(36) Smith, I. C. P. In *NMR of Newly Accessible Nuclei*; Laszlo, P., Ed.; Academic Press: London, 1983; Vol. 2; p 1.

(37) Jelinski, L. W. In *High-Resolution NMR Spectroscopy of Synthetic Polymers in Bulk (Methods and Stereochemical Analysis)*; Komoroski, R. A., Ed.; VCH Publishers: New York, 1986; Vol. 7; p 335.

(38) Barnes, R. G. *Adv. Nucl. Quadrupole Reson.* **1974**, *1*, 335.

(39) Stocktone, G. W.; Polnaszek, C. F.; Tulloch, A. P.; Hasan, F.; Smith, I. C. P. *Biochemistry* **1976**, *15*, 954−966.

(40) Waldstein, P.; Rabideau, S. W.; Jackson, J. A. *J. Chem. Phys.* **1964**, *41*, 3407−3411.

(41) Holcomb, D. F.; Pedersen, B. *J. Chem. Phys.* **1962**, *36*, 3270−3273.

(42) Vega, A. J.; Luz, Z. *J. Chem. Phys.* **1987**, *86*, 1803−1813.

(43) Spiess, H. W.; Sillescu, H. *J. Magn. Reson.* **1981**, *42*, 381−389.

(44) Spiess, H. W. In *Dynamic NMR Spectroscopy*; Springer-Verlag: Berlin, 1978; Vol. 15; pp 55−214.

(45) Torchia, D. A.; Szabo, A. *J. Magn. Reson.* **1982**, *49*, 107−121.

(46) Wittebort, R. J.; Olejniczak, E. T.; Griffin, R. G. *J. Chem. Phys.* **1987**, *86*, 5411−5420.

(47) Brown, G. M.; Noe-Spirlet, M.-R.; Busing, W. R.; Levy, H. A. *Acta Crystallogr., Sect. B* **1977**, *B33*, 1038−1046.

(48) Diercksen, G. H. F.; Kraemer, W. P.; Roos, B. O. *Theor. Chim. Acta* **1975**, *36*, 249−274.

(49) Silvidi, A. A. *J. Chem. Phys.* **1966**, *45*, 3892−3895.

(50) Mioc, U. B.; Colomban, P.; Davidovic, M.; Tomkinson, J. *J. Mol. Struct.* **1994**, *326*, 99−107.

(51) Polson, J. M.; Fyfe, J. D. D.; Jeffery, K. R. *J. Chem. Phys.* **1991**, *94*, 3381−3388.

(52) Pimentel, G. C.; McClellan, A. L. *The Hydrogen Bond*; Freeman: New York, 1960.